Dalton Transactions

ROYAL SOCIETY OF CHEMISTRY

PAPER

View Article Online
View Journal | View Issue

Cite this: *Dalton Trans.*, 2021, **50**, 6568

Meta-studtite stability in aqueous solutions. Impact of HCO_3^-, H_2O_2 and ionizing radiation on dissolution and speciation†

Junyi Li, * Zoltán Szabó and Mats Jonsson

Received 8th February 2021,
Accepted 8th April 2021

DOI: 10.1039/d1dt00436k

rsc.li/dalton

Two uranyl peroxides meta-studtite and studtite exist in nature and can form as alteration phases on the surface of spent nuclear fuel upon water intrusion in a geological repository. Meta-studtite and studtite have very low solubility and could therefore reduce the reactivity of spent nuclear fuel toward radiolytic oxidants. This would inhibit the dissolution of the fuel matrix and thereby also the spreading of radionuclides. It is therefore important to investigate the stability of meta-studtite and studtite under conditions that may influence their stability. In the present work, we have studied the dissolution kinetics of meta-studtite in aqueous solution containing 10 mM HCO_3^-. In addition, the influence of the added H_2O_2 and the impact of γ-irradiation on the dissolution kinetics of meta-studtite were studied. The results are compared to previously published data for studtite studied under the same conditions. ^{13}C NMR experiments were performed to identify the species present in aqueous solution (*i.e.*, carbonate containing complexes). The speciation studies are compared to calculations based on published equilibrium constants. In addition to the dissolution experiments, experiments focussing on the stability of H_2O_2 in aqueous solutions containing UO_2^{2+} and HCO_3^- were conducted. The rationale for this is that H_2O_2 was consumed relatively fast in some of the dissolution experiments.

Introduction

Storing spent nuclear fuel in deep geological repositories is at present the most probable method to permanently isolate high-level radioactive waste from the human environment.[1–4] Spent nuclear fuel from UO_2-based fuel contains approximately 95% UO_2. The remaining fraction is composed of fission products and heavier actinides.[5] These radionuclides have significantly higher specific radioactivity than the original fuel. Deep geological repository concepts are based on systems of barriers (natural and engineered) that will isolate the spent nuclear fuel from the environment until the radioactivity has reached levels comparable to uranium ore. In the event of a complete barrier failure in the repository, groundwater will be in contact with spent nuclear fuel.[6,7] This would provide the conditions necessary for spreading radioactivity to the biosphere. Fortunately, the UO_2-matrix has very low solubility in reducing groundwaters that are typically present in many potential repository sites.[8–10] Hence, the release of radionuclides incorporated in the UO_2-matrix could be assumed to be fairly slow. The inherent radioactivity of spent nuclear fuel will change the situation since the emitted ionizing radiation will induce radiolysis of the groundwater in contact with the fuel. The radiolysis of water produces oxidants ($HO^•$, $HO_2^•$ and H_2O_2) and reductants (e_{aq}^-, $H^•$ and H_2).[11,12] Kinetically, the oxidants will govern the chemistry at the fuel surface and drive the radionuclide release through the oxidative dissolution of the UO_2-matrix (U(VI) is much more soluble than U(IV)).[13] In general, groundwater contains HCO_3^- which forms strong soluble complexes with UO_2^{2+} and thereby facilitates matrix dissolution.[9,14] In certain situations (after glaciation), spent nuclear fuel might come in contact with water deficient in HCO_3^- ($<10^{-4}$ M).[15] Under these conditions radiolytically produced H_2O_2 may facilitate the formation of studtite ($(UO_2)O_2(H_2O)_4$) or its dehydrated counterpart meta-studtite ($(UO_2)O_2(H_2O)_2$). Kubatko[16] suggested that the alpha radiolysis of water gives a sufficient source of hydrogen peroxide in nature for uranyl peroxide mineral formation.

Studtite and meta-studtite[17,18] are the only known uranyl peroxide minerals in nature forming a class on their own.[16,19,20] Studtite was characterized as a secondary mineral of uranium on the surface of Chernobyl "lava". Hanson *et al.*[21] found the formation of studtite on the surface of spent nuclear fuel and meta-studtite at the sample air–water inter-

Department of Chemistry, School of Engineering Sciences in Chemistry, Biotechnology and Health, KTH Royal institute of Technology, SE-10044 Stockholm, Sweden. E-mail: ljunyi@kth.se

†Electronic supplementary information (ESI) available. See DOI: 10.1039/d1dt00436k

face after immersing commercial spent nuclear fuel particles in water over 2 years. It is important to note that the precipitation of studtite in solutions containing sufficient concentrations of H_2O_2 and U(VI) occurs at a temperature below 50 °C, while meta-studtite precipitates at a temperature above 70 °C.[19,20,22–24] A mixture of the two uranyl peroxides forms between 50 °C and 70 °C. The transformation between studtite and meta-studtite is irreversible, and occurs at 100 °C in air or at ambient temperature in a vacuum for 24 hours.[20,25–27] Recently, Spano[28] *et al.* thoroughly studied the phase transition temperatures of studtite to metastudtite and meta-studtite to UO_x. It is evident that the transition temperatures between them depend on the applied heating rate. They also proposed that the dehydration of studtite to metastudtite first occurs at particle surfaces and then progresses inward through geometrical contraction or diffusion-related kinetic models.[28]

Uranyl peroxides may form on nuclear fuel in a water-cooled reactor or in a wet interim storage system if the fuel cladding is damaged.[29–31] Under certain accident scenarios, the formation of uranyl peroxides must also be considered.[31]

Depending on the exposure history of spent nuclear fuel prior to its placement in a deep geological repository, studtite or meta-studtite could cover a part of the fuel surface. For this reason, the dissolution of studtite and meta-studtite in groundwater containing 2–10 mM HCO_3^- is a process that needs to be considered in the safety assessment of a deep geological repository for spent nuclear fuel.[15,32] In general, the solubility of studtite is very low in water, but considerably higher in solutions containing bicarbonate. This can be attributed to the formation of various soluble uranyl-carbonate or uranyl-peroxide-carbonate complexes. A recent study[17] demonstrated that studtite exposed to gamma radiation in HCO_3^- containing water dissolves quite readily. However, in this case studtite is decomposed radiolytically which results in uranium release. According to Amme,[33] studtite and meta-studtite have solubilities of 10^{-5} and 1.5×10^{-5} mol l^{-1}, respectively, at pH close to 7, indicating that meta-studtite dissolves more readily than studtite.

To the best of our knowledge, experimental data on the stability and dissolution kinetics of meta-studtite under geological repository conditions are still not available. Numerous studies have shown that uranyl forms soluble complexes with H_2O_2 and CO_3^{2-} in alkaline solutions or nanoclusters at pH ≥ 12.[34–40] However, the species formed in the dissolution of studtite or meta-studtite in the presence of HCO_3^- (at pH ≈ 9) have not been identified.

In this work, the dissolution dynamics of meta-studtite in aqueous solution was studied in the presence and absence of HCO_3^- to assess the impact of HCO_3^-. The released H_2O_2 and U(VI) were monitored as a function of time. In addition, the effect of added H_2O_2 and γ-radiation on the dissolution of meta-studtite in 10 mM HCO_3^- was studied. The results are compared to recently published data on studtite dissolution.[17] Furthermore, ^{13}C NMR spectroscopy was used to identify the carbonate-containing species formed in the dissolution experiments under the conditions mentioned above.

Experimental section

All solutions were prepared using Milli-Q water (18.2 MΩ cm), and all chemicals used were of reagent grade unless otherwise stated. Uranyl nitrate ($UO_2(NO_3)_2 \cdot 6H_2O$) and sodium bicarbonate ($NaHCO_3$) were used to prepare stock solutions which were diluted to the desired concentrations of HCO_3^- and U(VI) in the specific experiments.

The concentration of H_2O_2 was measured indirectly using the Ghormley triiodide method,[41,42] where I^- is oxidized to I_3^- by H_2O_2. The absorbance of I_3^- was measured at λ = 360 nm by UV/vis spectrophotometry.

The concentrations of U(VI) in solution were measured using the Arsenazo III method,[43] where uranyl reacts with the Arsenazo III reagent forming a complex in acidic media. The absorbance of the complex was measured at λ = 653 nm by UV/Vis spectrophotometry.

For each measurement of the H_2O_2 and U(VI) concentrations, analysis was performed in duplicate. The difference between the duplicate measurements was less than 4.5 μM and 14 μM, for H_2O_2 and U(VI), respectively. All experiments were performed at least three times. The error bars in the figures reflect the results of these experiments and are based on the standard deviation derived from the three repetitions of each experiment.

Synthesis of meta-studtite

For each individual experiment, a batch of 36 mg of meta-studtite powder was precipitated by adding 40 mM H_2O_2 to 4.3 mM uranyl nitrate in a total volume of 25 mL. An excess of H_2O_2 was used for maximizing the product formation. The uranyl solution was prepared by dissolving 54 mg of uranyl nitrate in a sample bottle containing 25 mL of water at an initial pH value of 3.5 acidified with HCl. The uranyl solution was sealed with a rubber septum and placed in a water bath heated to 90 °C, and then H_2O_2 was slowly added to the uranyl solution. The synthesis was carried out at 90 °C in a water bath with stirring for 3 hours. At this point the remaining concentration of U(VI) is less than 0.1 mM. After the synthesis, the meta-studtite suspension was left for 3 hours to completely sediment. The synthesized pale-yellow meta-studtite precipitate was washed twice with water to remove the remaining H_2O_2 and unreacted uranyl nitrate. During each washing step, the original liquid was replaced with 25 mL of water, and the suspension was left to re-sediment for 3 hours.

Solid phase characterization

Synthesized meta-studtite was characterized using powder X-ray diffraction (XRD). XRD patterns were recorded at room temperature using a PANalytical XPert PRO diffractometer using a Bragg–Brentano geometry and Cu Kα radiation (1.5418 Å) in a 2θ range between 10° and 80°. The powder sample was ground manually in an agate mortar.

Meta-studtite dissolution kinetics and the influence of added H_2O_2

After washing each 36 mg meta-studtite batch with water, the liquid was replaced with 25 mL of H_2O or an aqueous solution

containing 10 mM HCO_3^- and sealed with a rubber septum. Starting from immediately after adding the aqueous solution, the concentrations of H_2O_2 and U(VI) were measured as a function of time. The dissolution experiments were carried out at room temperature with continuous N_2 purging and stirring. For each H_2O_2 and U(VI) measurement, 1.2 mL aliquots were taken from the meta-studtite suspension and filtered through 0.2 μm cellulose acetate syringe filters.

The influence of H_2O_2 on the meta-studtite dissolution kinetics in 10 mM bicarbonate solutions was studied by adding H_2O_2 to a concentration of 0.2 mM at the beginning of the experiment. The pH of the solutions was measured before and after each experiment. No buffer was added to the solutions without added HCO_3^-.

Irradiation experiments

γ-Irradiation experiments were carried out after adding 25 mL of an aqueous solution containing 10 mM HCO_3^- to the washed meta-studtite powder. The glass vessels containing the suspensions were sealed with rubber septa and irradiated with a Cs-137 gamma source for 8 h with N_2 purging (Gammacell 1000 Elite, MDS Nordion). The dose rate of 0.11 Gy s^{-1} was determined by Fricke dosimetry.[11] The concentrations of H_2O_2 and U(VI) were measured before γ-radiation exposure and then every hour. Before each measurement, the suspensions were quickly shaken to ensure homogeneous sampling, and then 1.2 mL aliquots were taken from the suspensions. The pH values of the solutions were measured before and after exposure to ionizing radiation.

^{13}C NMR experiments

^{13}C NMR experiments were performed with a Bruker DMX-400 (54.2 MHz) spectrometer using a 10 mm normal broadband probe head without lock. The samples were prepared using ^{13}C enriched sodium bicarbonate (99% (CP), 98 atom % ^{13}C, Sigma-Aldrich). The spectra were measured at 0 °C using 10 mm NMR tubes which were tightly closed with a screwed cap in order to avoid the decomposition of the complexes and H_2O_2. The probe temperature was measured by using a calibrated Pt-100 resistance thermometer and adjusted using a Bruker Eurotherm variable temperature control unit. The samples were allowed to equilibrate to the specified temperature before the measurements. In order to obtain a satisfactory signal-to-noise ratio, the number of collected scans was varied between the experiments for the various test solutions.

For each NMR measurement in the dissolution experiments, 3 mL of the samples were taken after 48 hours. To minimize the influence of powders, the stirring was stopped during the final 12 hours of the experiment. In other speciation studies, 3 mL of the samples were also taken.

The conditions for all the experiments performed and discussed in this work (including previously published data for studtite)[17] are listed in Table 1 along with solution speciation obtained from ^{13}C NMR characterization.

Results and discussion

Solid phase characterization

In a recent paper[17] it was shown that when adding an excess amount of H_2O_2 to an aqueous uranyl nitrite solution at ambient temperature, the precipitate formed was pure studtite as confirmed by XRD. The meta-studtite powder was synthesized in this study by adding an excess amount of H_2O_2 to an aqueous uranyl nitrite solution at 85–90 °C (controlled by using a water bath). The precipitate formed showed a pale-yellow color and was confirmed to be meta-studtite by XRD. The color is in line with what has previously been reported in the literature[45,46] and the XRD pattern shown in Fig. 1 is in line with literature data.[44] The reason for performing the synthesis at elevated temperature instead of first synthesizing studtite and then drying it in air at high temperature to yield meta-studtite was to avoid uneven temperature distribution which could result in incomplete transformation or transformation to UO_x (amorphous) above 200 °C.[24,28,47]

Meta-studtite dissolution kinetics in pure water and 10 mM HCO_3^-

Similarly to studtite, meta-studtite has very low solubility in pure water.[17,48] In the meta-studtite dissolution experiments performed in pure water, the concentrations of U(VI) and H_2O_2 were very close to the detection limits of spectrophotometry (0.001 mM and 0.01 mM, respectively), therefore the measured values are quite ambiguous and cannot be evaluated.

Table 1 Test solutions for dissolution experiments and the complexes identified by ^{13}C NMR

	Dissolution conditions	Complexes identified by ^{13}C NMR[a]
Meta-studtite	Pure water	—
Meta-studtite	10 mM HCO_3^-	1, 2, 3
Meta-studtite	10 mM HCO_3^- + 0.2 mM added H_2O_2	1
Meta-studtite	10 mM HCO_3^- + γ-irradiation	1, 3
Studtite[b]	Pure water	—
Studtite[b]	10 mM HCO_3^-	1, 2, 3, 4
Studtite[b]	10 mM HCO_3^- + 0.2 mM added H_2O_2	1, 2, 3, 4
Studtite[b]	10 mM HCO_3^- + γ-irradiation	1, 3

[a] Numbers are referring to the structures in Scheme 1. [b] Samples studied previously in dissolution experiments in ref. 17.

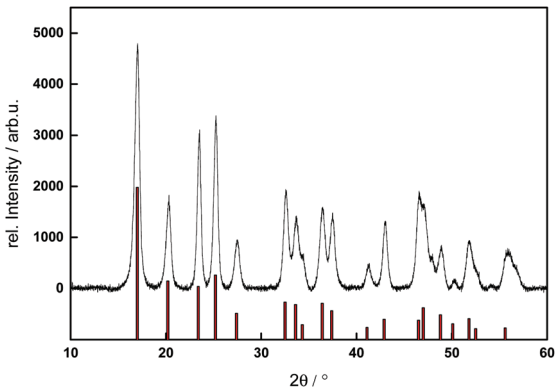

Fig. 1 Powder XRD pattern of synthesized meta-studtite (black) compared to ref. 44 (red).[44]

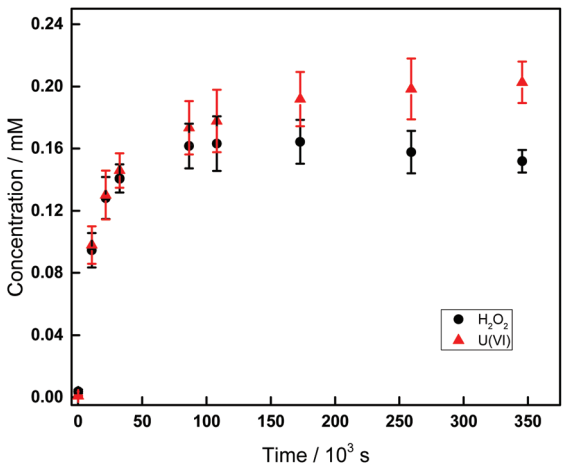

Fig. 2 Concentrations of H_2O_2 (black dots) and U(VI) (red triangles) as a function of time for aqueous meta-studtite powder suspensions containing 10 mM HCO_3^-.

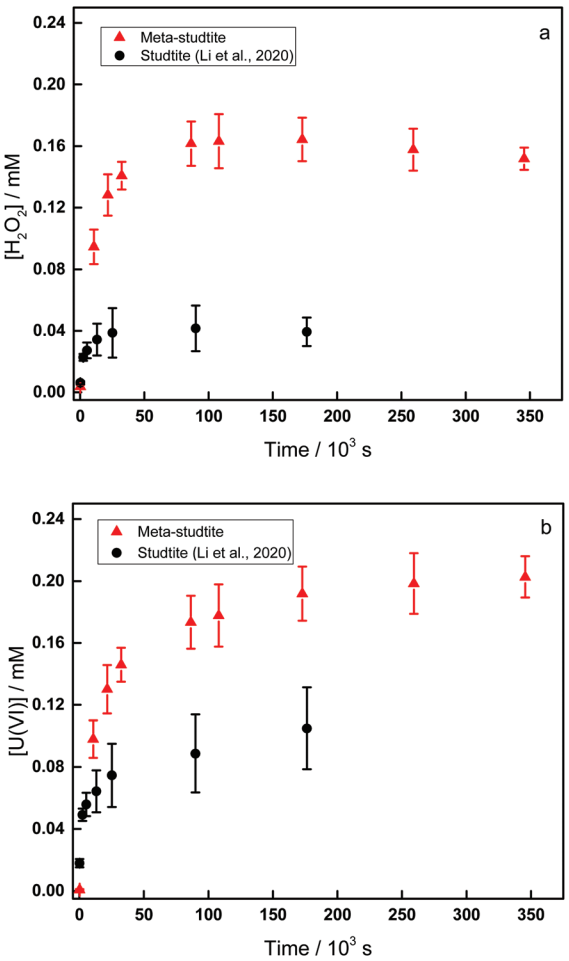

Fig. 3 $[H_2O_2]$ (a) and [U(VI)] (b) as a function of time for aqueous meta-studtite powder (red triangles) and studtite powder[17] (black dots) suspensions containing 10 mM HCO_3^-.

The results of the meta-studtite dissolution experiments in aqueous solutions containing 10 mM HCO_3^- are presented in Fig. 2. For comparison, the H_2O_2 and U(VI) concentrations are plotted separately in Fig. 3 including previously published data for studtite.[17] As carbonate enables the formation of soluble uranyl-carbonate and uranyl-peroxo-carbonate complexes, the solubility and the rate of meta-studtite and studtite dissolution are expected to increase with increasing carbonate concentration.[14,49–51]

As can be seen, meta-studtite is considerably more soluble than studtite. It is interesting to note that meta-studtite dissolves with almost equimolar amounts of H_2O_2 and U(VI) while this is not the case with studtite where the H_2O_2/U(VI) ratio is closer to 1 : 2. As previously observed in studtite dissolution experiments,[17] there is a slow decomposition of H_2O_2 also in the meta-studtite experiment. This slow decomposition of H_2O_2 seems to be accompanied by an equally slow increase in the U(VI) concentration which is in line with what can be expected from the solubility product. It can be seen that H_2O_2 is consumed more rapidly in the studtite system (at least in relative terms) than in the meta-studtite system. The ^{13}C NMR spectra for the solutions after 48 h of dissolution of studtite and meta-studtite are shown in Fig. 4.

Four carbonate containing complexes were identified in the studtite and meta-studtite dissolution experiments performed in this work. Their structures are shown in Scheme 1. Their identification is based on the comparison of their ^{13}C NMR chemical shifts to the shifts of complexes reported in a multinuclear study of the ternary uranium(VI)-peroxo-carbonato system.[35] The complexes and their ^{13}C NMR chemical shifts are $UO_2(CO_3)_3^{4-}$ (167.54 ppm) (**1**), $UO_2(O_2)(CO_3)_2^{4-}$ (166.92 ppm) (**2**), $(UO_2)_2(O_2)(CO_3)_4^{6-}$ (166.79 ppm) (**3**) and $UO_2(O_2)CO_3^{2-}$ (166.66 ppm) (**4**).

As can be seen, the first three complexes are present in both solutions, although with quite different ratios. Speciation calculations based on the stability constants of different complexes[35] show that the complexes identified in the ^{13}C NMR spectra are indeed the thermodynamically most stable ones under the given experimental conditions. The results of the speciation calculations are shown in Fig. 5.

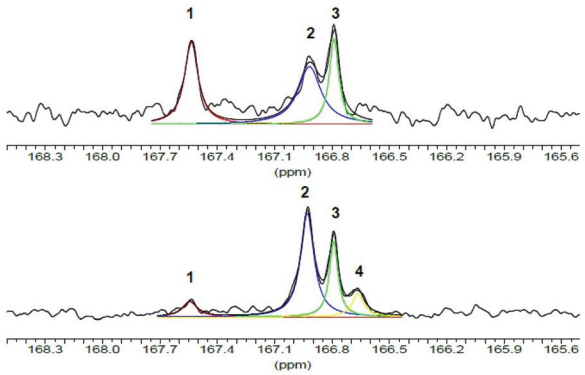

Fig. 4 ^{13}C NMR signals of the complexes formed in dissolution experiments of studtite (top) and meta-studtite (bottom) in solutions containing 10 mM HCO_3^-. The signal for free HCO_3^-/CO_3^{2-} is not shown. The vertical scale is arbitrary for the spectra.

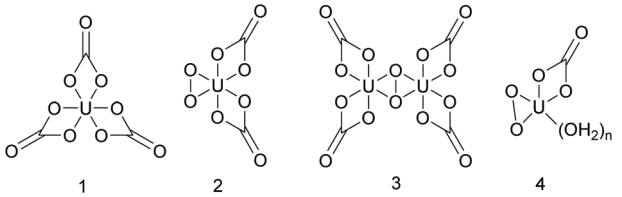

Scheme 1 Structure of the complexes identified by ^{13}C NMR spectroscopy in the various experiments, U = UO_2^{2+} (charges are neglected for simplicity) and n = 1, 2.

Meta-studtite dissolution kinetics in solutions containing H_2O_2

It was previously shown for studtite that significant dissolution is observed also in solutions containing H_2O_2.[17] The same type of experiment has now been performed for meta-studtite and the result is shown in Fig. 6 together with the previously published data for studtite.[17]

As can be seen, the initial presence of H_2O_2 suppresses the dissolution of meta-studtite slightly as was also shown for studtite. Then, the H_2O_2 concentration decreases with time for both meta-studtite and studtite. The corresponding ^{13}C NMR spectra for the solutions after 48 h of dissolution are shown in Fig. 7.

Due to the lower total uranium concentration, the signals are weaker than those observed in the dissolution experiments without added H_2O_2. The relative ratio between the complexes formed is also quite different. Speciation calculations (ESI, Fig. S3 and S4†) based on the stability constants of the different complexes show again that the complexes identified with NMR are indeed the thermodynamically most stable complexes under the given conditions.[35]

H_2O_2 stability

In order to further elucidate the reason behind the observed consumption of H_2O_2 in the dissolution experiments we have conducted a series of experiments where the H_2O_2 concentrations have been monitored as a function of time in solutions containing 10 mM HCO_3^- and uranyl concentrations ranging from 0 to 0.4 mM. Three sets of experiments were performed with different initial H_2O_2 concentrations (0.1–0.3 mM). The concentrations of H_2O_2 and U(VI) were monitored initially and after every 24 hours for a total of 96 hours. The pH values were measured before and after each experiment. The experiments were carried out at room temperature without stirring and purging. Each sample container was sealed and protected from light. The results (H_2O_2 concentration *vs.* time and the H_2O_2 consumption rate as a function of uranyl concentration) are plotted in Fig. 8–10. It should be noted that there was no precipitate formed, and the uranyl concentration remained constant with time in all experiments.

Fig. 8a, 9a and 10a show that the H_2O_2 concentration decreases with time and that the rate of consumption is strongly dependent on the concentration of uranyl. It can be seen that the rate of H_2O_2 consumption increases with increasing initial concentration of H_2O_2. Fig. 8b–10b show the rate of H_2O_2 consumption as a function of the concentration of uranyl. As we can see the maximum rate of H_2O_2 consumption is observed at around 0.2 mM U(VI) regardless of the initial

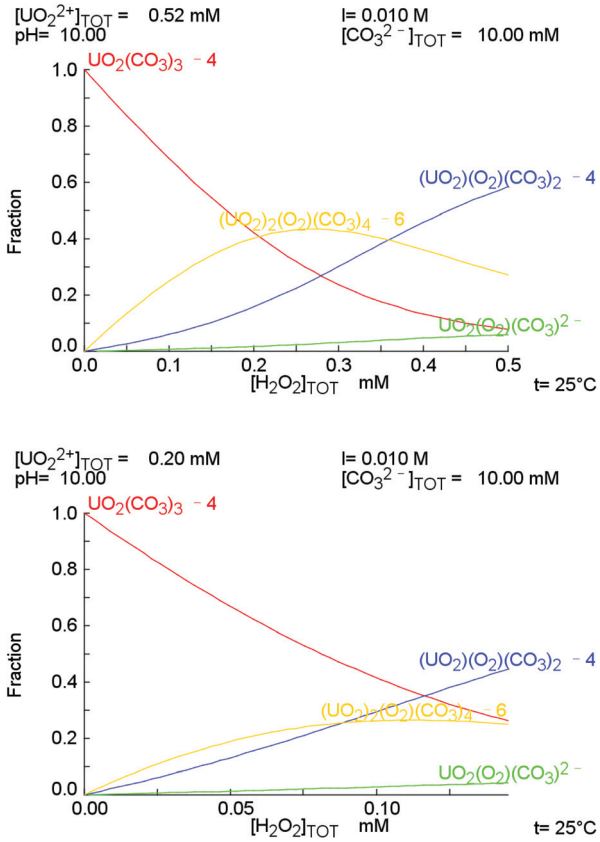

Fig. 5 Plot of the uranyl fraction *vs.* total peroxide concentration calculated by Medusa using the equilibrium constants reported for the complexes formed in the ternary U(VI)-peroxide-carbonate system (left).[35] The effect of ionic strength (I = 0.01 mol kg^{-1} (H_2O)) was accounted for using the simplified HKF (Helgeson–Kirkham–Flowers) model.[52–54]

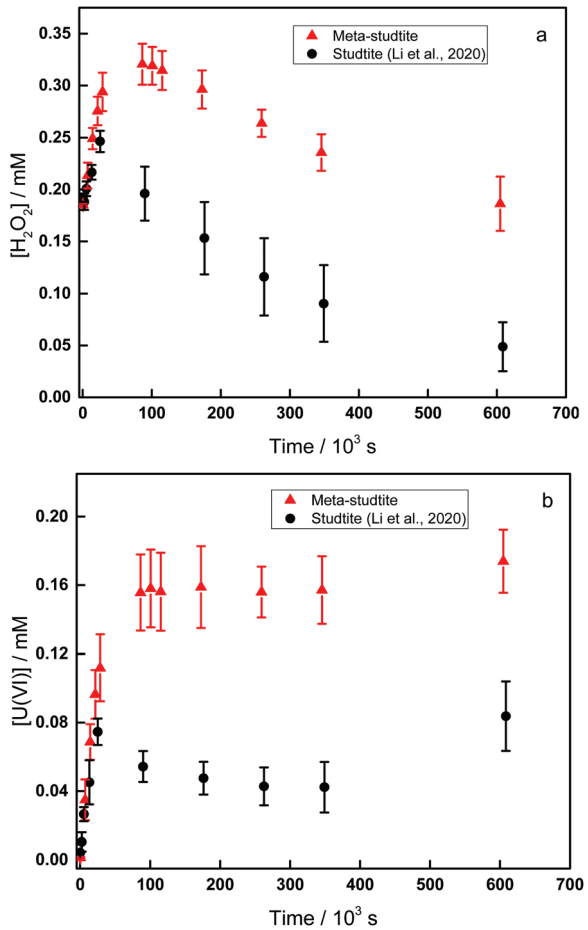

Fig. 6 $[H_2O_2]$ (a) and [U(VI)] (b) as a function of time for aqueous meta-studtite powder (red triangles) and studtite powder[17] (black dots) suspensions containing 10 mM added HCO_3^- and 0.2 mM H_2O_2.

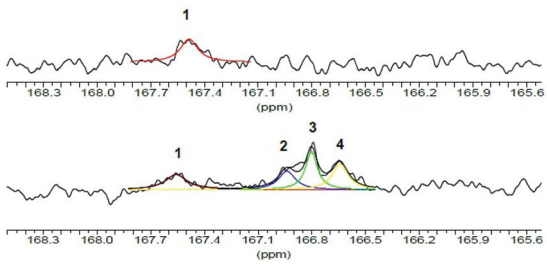

Fig. 7 ^{13}C NMR signals of the complexes formed in dissolution experiments of studtite (top) and meta-studtite (bottom) in solutions containing 10 mM HCO_3^- in the presence of added H_2O_2. The vertical scale is arbitrary for the spectra.

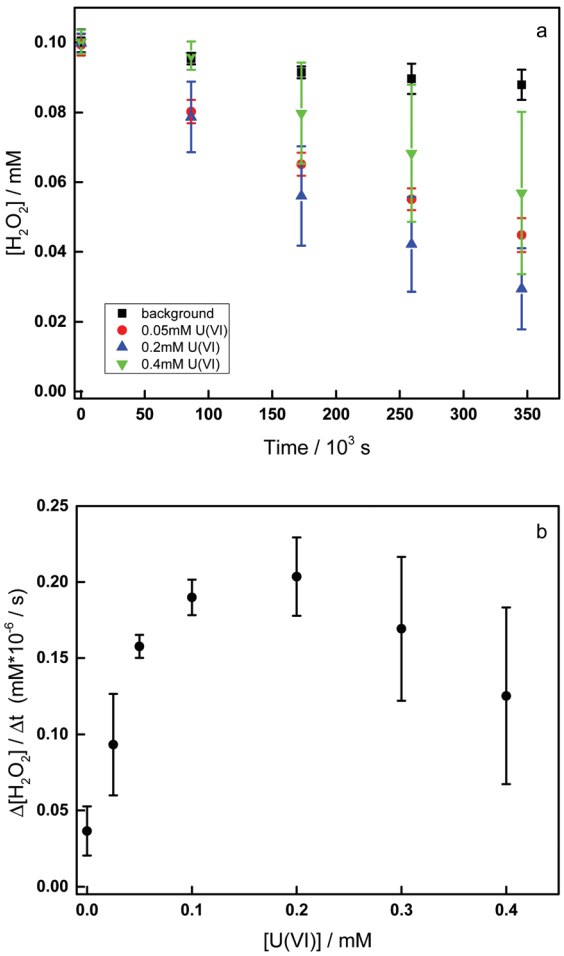

Fig. 8 (a) Concentration of H_2O_2 as a function of time for 0.1 mM H_2O_2 decomposition in 10 mM HCO_3^- and different concentrations of U(VI). (b) The average decomposition rate of 0.1 mM H_2O_2 in 10 mM HCO_3^- and different concentrations of U(VI) after 96 h *vs.* different concentrations of U(VI).

H_2O_2 concentration. The only variable factor in the three systems is the concentration of uranyl. If uranyl only promotes the consumption of H_2O_2, one would expect a correlation between the concentration of uranyl and the consumption rate of H_2O_2. However, the fact that there seems to be an optimum uranyl concentration implies that the impact of uranyl is more complicated which is quite intriguing. To shed some more light on this, the ^{13}C NMR spectra for a solution containing 0.3 mM U(VI), 0.3 mM H_2O_2 and 10 mM HCO_3^- and a solution containing 0.5 mM U(VI), 0.3 mM H_2O_2 and 10 mM HCO_3^- were recorded immediately after preparation and after one week. The results are shown in Fig. 11.

Based on the NMR spectra, it is obvious that the speciation changes with time and the initial and final compositions of the test solutions differ significantly. The species observed in the solutions after one week are identical to the thermodynamically most stable complexes as indicated by the speciation (Fig. S5†) calculated for the initial conditions as the NMR-spectra were recorded. However the initial compositions of both solutions are very different from the calculated ones and the NMR spectra show that only one complex, $UO_2(O_2)(CO_3)_2^{4-}$, is formed initially. Hence, the formation of this complex is kinetically favored.

Fig. 8–10 show that U(VI) appears to catalyze the decomposition of H_2O_2 in these systems. The somewhat complex U(VI) concentration dependence could be attributed to the fact that

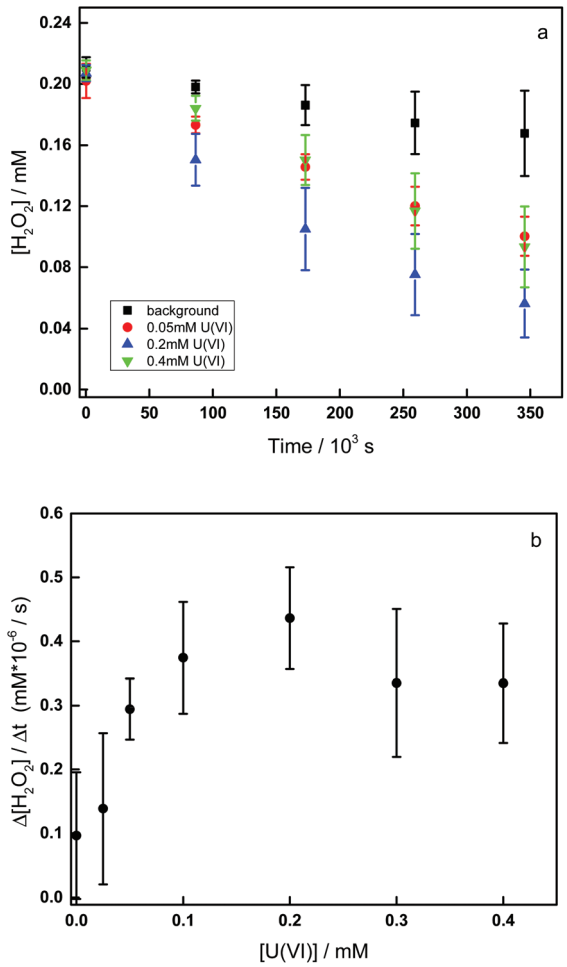

Fig. 9 (a) Concentration of H_2O_2 as a function of time for 0.2 mM H_2O_2 decomposition in 10 mM HCO_3^- and different concentrations of U(VI). (b) The average decomposition rate of 0.2 mM H_2O_2 in 10 mM HCO_3^- and different concentrations of U(VI) after 96 h *vs.* different concentrations of U(VI).

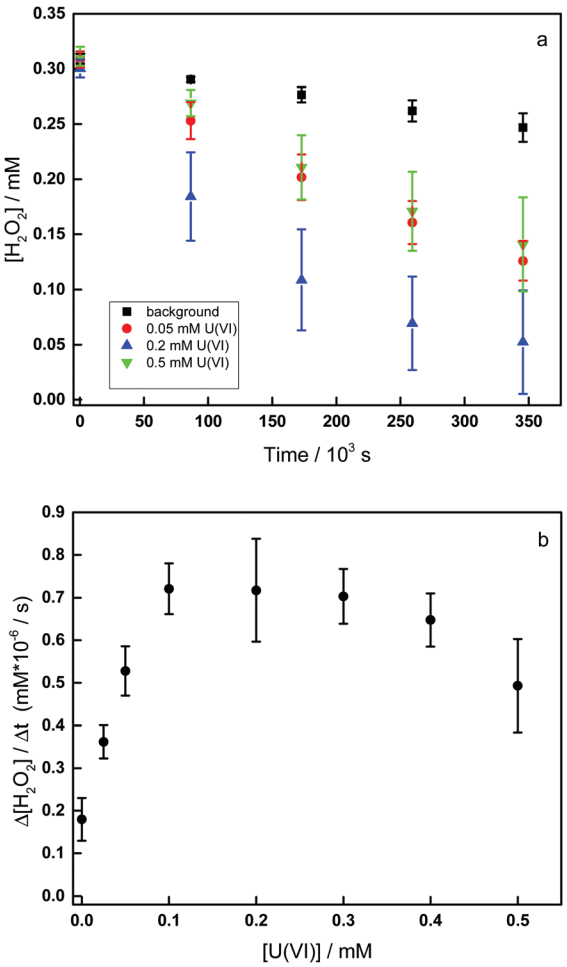

Fig. 10 (a) Concentration of H_2O_2 as a function of time for 0.3 mM H_2O_2 decomposition in 10 mM HCO_3^- and different concentrations of U(VI). (b) The average decomposition rate of 0.3 mM H_2O_2 in 10 mM HCO_3^- and different concentrations of U(VI) after 96 h *vs.* different concentrations of U(VI).

the main peroxide species at higher U(VI) concentrations is $(UO_2)_2(O_2)(CO_3)_4^{6-}$ which might be less sensitive to catalytic decomposition. Therefore we initially (at low U(VI)-concentrations) observed a positive correlation with the U(VI)-concentration (*i.e.* the rate of decomposition increases with increasing U(VI)-concentration). At a certain U(VI)-concentration, the stabilizing effect of $(UO_2)_2(O_2)(CO_3)_4^{6-}$ will become dominating and the rate of H_2O_2 decomposition will start to decrease with increasing U(VI)-concentration.

To elucidate the mechanism of the catalytic decomposition of H_2O_2, a radical scavenging experiment using 200 mM CH_3OH was performed. Upon reaction with a hydroxyl radical, CH_3OH produces formaldehyde which can be detected spectrophotometrically. This has been used successfully to detect hydroxyl radicals formed in the catalytic decomposition of H_2O_2 on oxide surfaces. However, in the present case, no detectable amount of formaldehyde was observed. Therefore, we conclude that hydroxyl radicals are not formed during the process.[55] The exact mechanism of the catalytic decomposition of H_2O_2 in this system has not been confirmed.

Gamma-irradiation experiment

The results of the dissolution experiments performed under exposure to gamma-radiation are presented in Fig. 12.

As can be seen, meta-studtite is also dissolved when exposed to gamma radiation. The U(VI) concentration increases beyond what is seen in the conventional dissolution experiments. Just as was previously observed for studtite, the concentration of U(VI) is significantly higher than the concentration of H_2O_2 which implies that the mechanism is similar. Indeed, in a continuously gamma-irradiated aqueous solution, H_2O_2 reaches a steady-state fairly rapidly since there are several reactions that consume radiolytically produced H_2O_2.[56] Therefore, the concentration of H_2O_2 in pure irradiated water is not really expected to exceed 10^{-6} M.[11] The meta-studtite contributes significantly to H_2O_2 upon dissolution and the imbalance

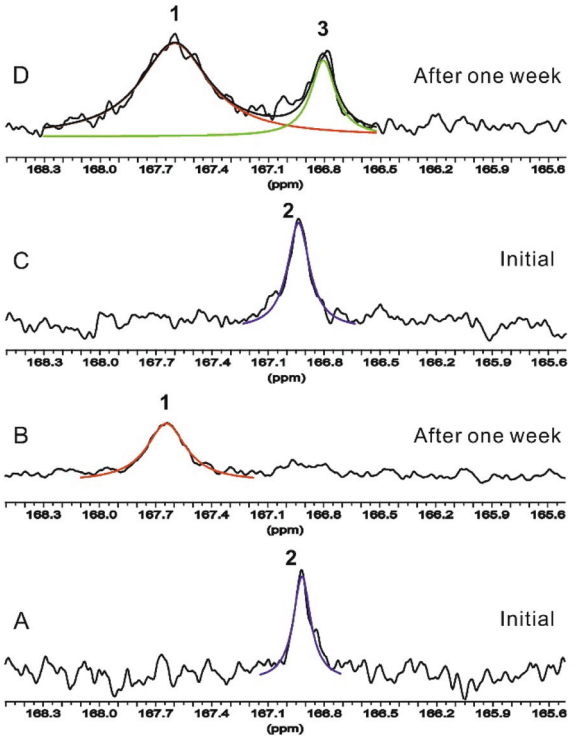

Fig. 11 ^{13}C NMR signals of the complexes formed in solutions containing 0.3 mM H_2O_2, 10 mM HCO_3^- and 0.3 mM U(VI) (A) and (B) or 0.5 mM U(VI) (C) and (D). Spectra (A) and (C) were measured immediately after sample preparation, and spectra (B) and (D) were measured using the same samples after one week. The vertical scale is arbitrary for the spectra.

between H_2O_2 and U(VI) in solution is attributed to the radiolytic consumption of H_2O_2. For comparison, we also recorded the ^{13}C NMR spectra for the solutions after irradiation (Fig. 13).

The complexes identified by NMR are $UO_2(CO_3)_3^{4-}$ (1) and $(UO_2)_2(O_2)(CO_3)_4^{6-}$ (3). The ratio between these two complexes appears to be the same within the experimental uncertainty, 1 : 0.23 and 1 : 0.19 for studtite and meta-studtite, respectively. The identified dominant complexes are in good agreement with the speciation calculations under the same conditions (Fig. 14).

As has previously been shown for studtite, the high U(VI) concentrations obtained upon irradiation of the aqueous meta studtite suspensions containing HCO_3^- can most probably be explained by the increase in pH throughout the experiment (from initial 8.8 to final 9.9) which drastically increases the stability of some of the uranyl-peroxo-carbonate complexes and thereby reduces the concentration of free H_2O_2 to very low levels. The direct consequence of this is that the solubility of meta-studtite increases. Hence, the combination of the radiolytic degradation of H_2O_2 and the formation of uranyl-peroxo-carbonate complexes maintains the concentration of free H_2O_2 at a very low level and thereby drives the dissolution process. The direct consequence of this is that studtite and meta-studtite present on the surface of spent nuclear fuel in a deep geological repository are readily dissolved upon groundwater

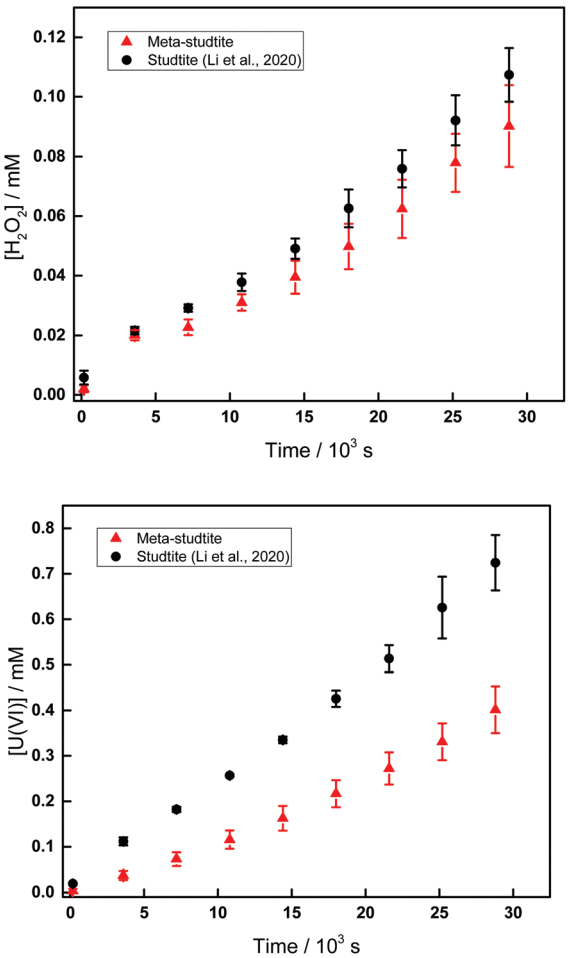

Fig. 12 Concentration of H_2O_2 (a) and U(VI) (b) as a function of time for irradiated aqueous meta-studtite powder (red triangles) and studtite powder[17] (black dots) powder suspensions containing 10 mM HCO_3^-.

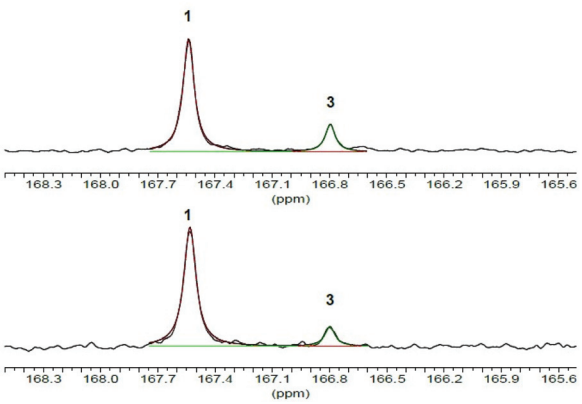

Fig. 13 ^{13}C NMR signals of the complexes formed in dissolution experiments of studtite (top) and meta-studtite (bottom) in solutions containing 10 mM HCO_3^- with gamma-irradiation. The vertical scale is arbitrary for the spectra.

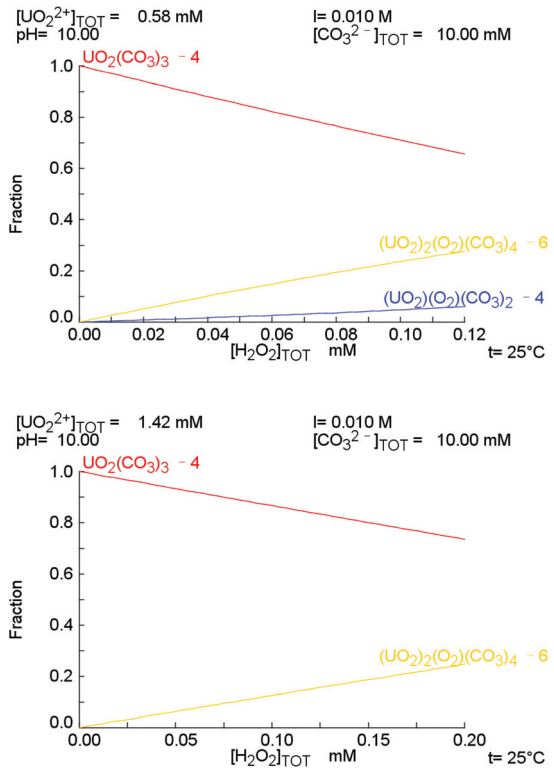

Fig. 14 Plot of the uranyl fraction *vs.* total peroxide concentration calculated by Medusa using the equilibrium constants reported for the complexes formed in the ternary U(VI)-peroxide-carbonate system (left).[35] The effect of ionic strength (I = 0.01 mol kg^{-1} (H_2O)) was accounted for using the simplified HKF (Helgeson–Kirkham–Flowers) model.[52–54]

intrusion and do not provide the protection of the fuel surface that the generally low solubility would imply.

Conclusions

This work shows that the solubility of meta-studtite in the suspensions without added HCO_3^- is, as expected, very low. In suspensions containing 10 mM HCO_3^-, the observed solubility is considerably higher and also higher than what was previously observed for studtite under the same conditions. The higher solubility in HCO_3^- containing solutions is attributed to the formation of uranyl-carbonate and uranyl-peroxo-carbonate complexes. The formation of these species is confirmed by the ^{13}C NMR studies and is in general in good agreement with what can be expected from thermodynamical data.

The solubility of meta-studtite in the presence of H_2O_2 (in HCO_3^- containing solutions) is lower than that in the absence of H_2O_2. It is obvious that H_2O_2 is consumed in systems where meta-studtite and studtite are dissolved. Additional experiments show that H_2O_2 is catalytically decomposed in solutions containing UO_2^{2+} and HCO_3^- where an optimum UO_2^{2+} concentration was found. The decomposition appears to follow a non-radical mechanism.

Upon exposure to γ-radiation, meta-studtite rapidly dissolves in an aqueous suspension containing 10 mM HCO_3^-. However, the rate of dissolution is lower than that of studtite under the same conditions. The rapid dissolution is attributed to a combination of the radiolytic degradation of H_2O_2 and the formation of uranyl-peroxo-carbonate complexes, maintaining the concentration of free H_2O_2 at a very low level and thereby driving the dissolution.

Author contributions

Conceptualization: J. L. and M. J.; data curation: J. L. and Z. S.; formal analysis: J. L., Z. S. and M. J.; funding acquisition: Z. S. and M. J.; investigation: J. L. and Z. S.; methodology: J. L. and M. J.; supervision: M. J.; writing – original draft: J. L.; writing – review & editing: J. L., Z. S. and M. J.

Conflicts of interest

The authors declare no conflict of interest.

Acknowledgements

The Swedish Nuclear Fuel and Waste Management Company (SKB) and the China Scholarship Council (CSC) are gratefully acknowledged for financial support.

Notes and references

1 J. O. Lee, H. Choi and G. Y. Kim, *Int. J. Heat Mass Transfer*, 2017, **115**, 192–204.
2 H. P. Berg and P. Brennecke, in *Managing Nuclear Projects*, Elsevier Ltd., 2013, pp. 152–174.
3 M. Jonsson, *ISRN Mater. Sci.*, 2012, **2012**, 1–13.
4 Ž. Veinović, B. K. Zelić and D. Domitrović, in *Handbook of Research on Advancements in Environmental Engineering*, IGI Global, 2014, pp. 367–399.
5 H. Kleykamp, *J. Nucl. Mater.*, 1985, **131**, 221–246.
6 Å. Björkbacka, C. M. Johnson, C. Leygraf and M. Jonsson, *J. Electrochem. Soc.*, 2017, **164**, C201–C206.
7 M. Jonsson, *Isr. J. Chem.*, 2014, **54**, 292–301.
8 D. W. Shoesmith, *J. Nucl. Mater.*, 2000, **282**, 1–31.
9 I. Grenthe, D. Ferri, F. Salvatore and G. Riccio, *J. Chem. Soc., Dalton Trans.*, 1984, 2439–2443.
10 A. S. Kertes and R. Guillaumont, *Nucl. Chem. Waste Manage.*, 1985, **5**, 215–219.
11 J. Spinks, *An introduction to radiation chemistry*, Wiley, New York, 3rd edn, 1990.
12 S. Nilsson and M. Jonsson, *J. Nucl. Mater.*, 2011, **410**, 89–93.
13 E. Ekeroth, O. Roth and M. Jonsson, *J. Nucl. Mater.*, 2006, **355**, 38–46.

14 C. Nguyen-Trung, G. M. Begun and D. A. Palmer, *Aqueous Uranium Complexes. 2. Raman Spectroscopic Study of the Complex Formation of the Dioxouranium(VI) Ion with a Variety of Inorganic and Organic Ligands*, 1992, vol. 31.
15 S. Kärnbränslehantering, *Svensk Kärnbränslehantering AB Data report for the safety assessment SR-Site*, 2010.
16 K. A. H. Kubatko, K. B. Helean, A. Navrotsky and P. C. Burns, *Science*, 2003, **302**, 1191–1193.
17 J. Li, A. C. Maier and M. Jonsson, *ACS Appl. Energy Mater.*, 2020, **3**, 352–357.
18 F. Clarens, J. De Pablo, I. Díez-Perez, I. Casas, J. Gimenez and M. Rovira, *Environ. Sci. Technol.*, 2004, **38**, 6656–6661.
19 A. Rey, I. Casas, J. Giménez, J. Quiñones and J. de Pablo, *J. Nucl. Mater.*, 2009, **385**, 467–473.
20 P. F. Weck and E. Kim, *J. Phys. Chem. C*, 2016, **120**, 16553–16560.
21 B. Hanson, B. McNamara, E. Buck, J. Friese, E. Jenson, K. Krupka and B. Arey, *Radiochim. Acta*, 2005, **93**, 159–168.
22 P. C. Debets, *J. Inorg. Nucl. Chem.*, 1963, **25**, 727–730.
23 E. H. P. Cordfunke and A. A. Van Der Giessen, *J. Inorg. Nucl. Chem.*, 1963, **25**, 553–555.
24 R. Thomas, M. Rivenet, E. Berrier, I. de Waele, M. Arab, D. Amaraggi, B. Morel and F. Abraham, *J. Nucl. Mater.*, 2017, **483**, 149–157.
25 T. Sato, *Naturwissenschaften*, 1961, **48**, 668.
26 T. Sato, *J. Appl. Chem.*, 2007, **13**, 361–365.
27 T. Sato, *Naturwissenschaften*, 1961, **48**, 693.
28 T. L. Spano, J. L. Niedziela, A. E. Shields, J. McFarlane, A. Zirakparvar, Z. Brubaker, R. J. Kapsimalis and A. Miskowiec, *J. Phys. Chem. C*, 2020, **124**, 26699–26713.
29 J. Abrefah, S. C. Marschman and E. D. Jenson, *Pacific Northwest National Laboratory Examination of the Surface Coatings Removed from K-East Basin Fuel Elements*, 1998.
30 C. R. Armstrong, M. Nyman, T. Shvareva, G. E. Sigmon, P. C. Burns and A. Navrotsky, *Proc. Natl. Acad. Sci. U. S. A.*, 2012, **109**, 1874–1877.
31 P. C. Burns, R. C. Ewing and A. Navrotsky, *Science*, 2012, **335**, 1184–1188.
32 J. A. T. Smellie, M. Laaksoharju and P. Wikberg, *J. Hydrol.*, 1995, **172**, 147–169.
33 M. Amme, *Radiochim. Acta*, 2002, **90**, 399–406.
34 P. L. Zanonato, P. Di Bernardo, V. Vallet, Z. Szabó and I. Grenthe, *Dalton Trans.*, 2015, **44**, 1549–1556.
35 P. L. Zanonato, P. Di Bernardo, Z. Szabó and I. Grenthe, *Dalton Trans.*, 2012, **41**, 11635–11641.
36 P. L. Zanonato, P. Di Bernardo and I. Grenthe, *Dalton Trans.*, 2012, **41**, 3380–3386.
37 H. L. Lobeck, J. K. Isner and P. C. Burns, *Inorg. Chem.*, 2019, **58**, 6781–6789.
38 P. Miró, S. Pierrefixe, M. Gicquel, A. Gil and C. Bo, *J. Am. Chem. Soc.*, 2010, **132**, 17787–17794.
39 G. E. Sigmon and P. C. Burns, *J. Am. Chem. Soc.*, 2011, **133**, 9137–9139.
40 P. C. Burns and M. Nyman, *Dalton Trans.*, 2018, **47**, 5916–5927.
41 W. A. Patrick and H. B. Wagner, *Anal. Chem.*, 1949, **21**, 1279–1280.
42 J. A. Ghormley and A. C. Stewart, *J. Am. Chem. Soc.*, 1956, **78**, 2934–2939.
43 S. B. Savvin, *Talanta*, 1961, **8**, 673–685.
44 P. F. Weck, E. Kim, C. F. Jové-Colón and D. C. Sassani, *Dalton Trans.*, 2012, **41**, 9748–9752.
45 M. Deliens and P. Piret, *Am. Mineral.*, 1983, **68**, 456–458.
46 X. Guo, D. Wu, H. Xu, P. C. Burns and A. Navrotsky, *J. Nucl. Mater.*, 2016, **478**, 158–163.
47 X. Guo, S. V. Ushakov, S. Labs, H. Curtius, D. Bosbach and A. Navrotsky, *Proc. Natl. Acad. Sci. U. S. A.*, 2014, **111**, 17737–17742.
48 J. Giménez, J. De Pablo, I. Casas, X. Martínez-Lladó, M. Rovira and A. Martínez Torrents, *Appl. Geochem.*, 2014, **49**, 42–45.
49 D. Gorman-Lewis, P. C. Burns and J. B. Fein, *J. Chem. Thermodyn.*, 2008, **40**, 335–352.
50 S. O. Odoh and G. Schreckenbach, *Inorg. Chem.*, 2013, **52**, 5590–5602.
51 I. Pashalidis, K. R. Czerwinski, T. Fanghänel and J. I. Kim, *Radiochim. Acta*, 1997, **76**, 55–62.
52 H. C. Helgeson, D. H. Kirkham and G. C. Flowers, *Am. J. Sci.*, 1981, **281**, 1249–1516.
53 E. H. Oelkers and H. C. Helgeson, *Geochim. Cosmochim. Acta*, 1990, **54**, 727–738.
54 E. L. Shock, E. H. Oelkers, J. W. Johnson, D. A. Sverjensky and H. C. Helgeson, *J. Chem. Soc., Faraday Trans.*, 1992, **88**, 803–826.
55 Q. Li, P. Sritharathikhun and S. Motomizu, *Anal. Sci.*, 2007, **23**, 413–417.
56 G. V. Buxton, C. L. Greenstock, W. P. Helman and A. B. Ross, *J. Phys. Chem. Ref. Data*, 1988, **17**, 513–886.